PAPER

Novel nanofluidic chemical cells based on self-assembled solid-state SiO$_2$ nanotubes

To cite this article: Hao Zhu *et al* 2017 *Nanotechnology* **28** 435601

View the article online for updates and enhancements.

Novel nanofluidic chemical cells based on self-assembled solid-state SiO₂ nanotubes

Hao Zhu[1,6,7], Haitao Li[2,3,6], Joseph W F Robertson[2], Arvind Balijepalli[2], Sergiy Krylyuk[4,5], Albert V Davydov[5], John J Kasianowicz[2], John S Suehle[2,7] and Qiliang Li[2,3,7]

[1] State Key Laboratory of ASIC and System, School of Microelectronics, Fudan University, Shanghai 200433, People's Republic of China
[2] Engineering Physics Division, National Institute of Standards and Technology, Gaithersburg, MD 20899, United States of America
[3] Department of Electrical and Computer Engineering, George Mason University, Fairfax, VA 22030, United States of America
[4] Theiss Research, La Jolla, CA 92037, United States of America
[5] Materials Science and Engineering Division, National Institute of Standards and Technology, Gaithersburg, MD 20899, United States of America

E-mail: hao_zhu@fudan.edu.cn, john.suehle@nist.gov and qli6@gmu.edu

Abstract

Novel nanofluidic chemical cells based on self-assembled solid-state SiO₂ nanotubes on silicon-on-insulator (SOI) substrate have been successfully fabricated and characterized. The vertical SiO₂ nanotubes with a smooth cavity are built from Si nanowires which were epitaxially grown on the SOI substrate. The nanotubes have rigid, dry-oxidized SiO₂ walls with precisely controlled nanotube inner diameter, which is very attractive for chemical-/bio-sensing applications. No dispersion/aligning procedures were involved in the nanotube fabrication and integration by using this technology, enabling a clean and smooth chemical cell. Such a robust and well-controlled nanotube is an excellent case of developing functional nanomaterials by leveraging the strength of top-down lithography and the unique advantage of bottom-up growth. These solid, smooth, clean SiO₂ nanotubes and nanofluidic devices are very encouraging and attractive in future bio-medical applications, such as single molecule sensing and DNA sequencing.

Supplementary material for this article is available online

Keywords: solid-state, SiO₂ nanotube, self-assembly, nanofluidic cell, *in-situ* fabrication, silicon-on-insulator

(Some figures may appear in colour only in the online journal)

1. Introduction

Since the first introduction of one-dimensional nanochannels/nanopores for single molecule detection, there has been increasing interest in modern nanofluidic system applications, e.g., ultra-fast DNA sequencing [1–4]. The recently developed artificial inorganic nanotubes have attracted certain attention due to their robustness of solid-state membranes, high aspect ratio, good mechanical properties, precise control of the nanotube size, and feasibility of surface functionalization [5–10]. In general, a typical solid-state nanotube has a length in microns and a diameter from 10–100 nm. The high aspect ratio enables the confinement of an entire molecule, which can give rise to new precise detection and translocation characteristics. In addition, the inorganic nanotubes (e.g., SiO₂) usually have hydrophilic surface that are accessible for various functionalization. Currently, solid-state nanotubes

---

[6] These authors contributed equally to this work.
[7] Authors to whom any correspondence should be addressed.

1
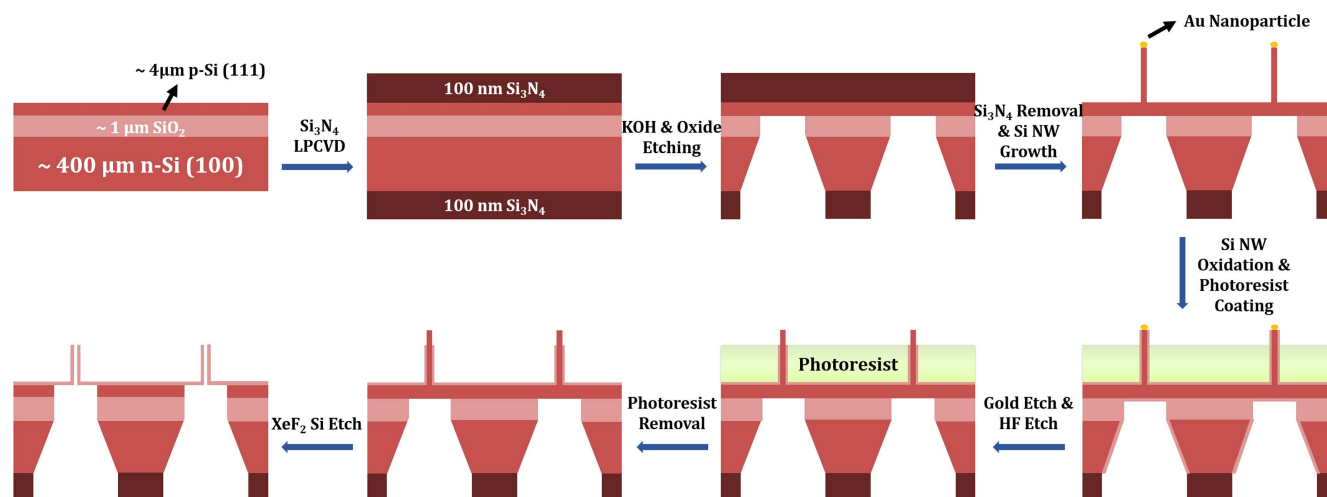
Figure 1. Process flow of the fabrication of SiO$_2$ nanotubes on SOI substrate from epitaxial Si nanowires.

were implemented in chemical-/bio-sensing applications, such as small molecule study, DNA translocation and sequencing [11–14].

Usually conventional preparation of SiO$_2$ nanotubes follows the template-assisted sol-gel route, whereas the inorganic nanotubes are synthesized within the nanopores of a porous membrane, e.g., alumina and polycarbonate [15–17]. Although using the alumina template is a technologically simple process, the nanotubes usually have poor morphology and porous walls. In addition, these nanotubes are easily damaged during the elimination process of the alumina membrane. Using polycarbonate and other porous membranes has similar drawbacks. A promising route to prepare robust SiO$_2$ nanotubes has been demonstrated by partial oxidation of vertical Si nanowires which are epitaxially grown on Si (111) surfaces and etching out the core [18, 19]. The SiO$_2$ nanotubes are then assembled into a microfluidic device after dispersion and alignment that involve additional microfabrication steps. Many of these steps will deteriorate the nanotube morphology, contaminate the inner wall and limit the ability to scale-up devices into massively parallel systems. In this work, we report a new and optimized process route to fabricate clean and smooth SiO$_2$ nanotubes on silicon-on-insulator (SOI) substrate with a cavity towards direct chemical-/bio-sensing devices. The inner diameter of the nanotube can be precisely controlled and scaled down to as small as 20 nm through multiple oxidation-etching processes. In addition, nanofluidic devices can be readily and precisely prepared by opening the nanochannel between the nanotube and SOI substrate using dry etching. No solution-based dispersion, transfer or aligning steps were involved, effectively protecting the naturally passivated SiO$_2$ nanotube surface. Such an optimized SiO$_2$ nanotube fabrication is very promising for robust nanofluidic device arrays and systems.

2. Experimental

The detailed process of fabricating SiO$_2$ nanotubes is illustrated in figure 1. The SOI substrate used here consists of a

400 μm handle Si (100) layer and a 4 μm top Si (111) layer with a sandwiched 1 μm buried oxide. The fabrication begins with a uniform deposition of 200 nm Si$_3$N$_4$ on both sides of the SOI wafer by low-pressure chemical vapor deposition. Then, squares of different sizes on the back Si$_3$N$_4$/Si (100) surface are defined by photolithography and the exposed Si$_3$N$_4$ is removed using reactive ion etching (RIE). This is followed by an anisotropic etching of Si (100) in a 30% w/w potassium hydroxide (KOH) solution at 85 °C for 6–7 h, with the patterned Si$_3$N$_4$ functioning as hard mask. The wet etching creates a cavity in the Si (100) layer with a trapezoidal cross-section that forms a 54.7° angle with the surface [20]. The KOH etching is terminated when reaching the buried oxide which has a much slower etch rate (1–2 orders of magnitude less) than Si (100). The substrate is then immersed in hydrofluoric (HF) acid to etch off the buried oxide on top of the opened square window, so that the Si (111) layer is exposed and suspended. After that, the top Si$_3$N$_4$ layer on Si (111) surface is removed by RIE.

The next step is the epitaxial synthesis of Si nanowire on the top Si (111) layer. The vapor–liquid–solid growth of Si nanowires was carried out in a custom-built hot wall CVD system at 900 °C and a reactor pressure of 80 kPa using 30 sccm of silicon tetrachloride (SiCl$_4$) and 200 sccm of hydrogen further diluted with nitrogen to a total flow rate of 1000 sccm [21, 22]. Commercially available Au nanoparticles of different diameter deposited on the poly-L-lysine-functionalized Si (111) surface were used to catalyze the growth. During the heating, the Au catalyst forms liquid Au–Si eutectic droplets by reacting with the Si substrate. When exposed to a SiCl$_4$/H$_2$ mixture, the droplets eventually become supersaturated by absorbing Si atoms from the arriving SiCl$_4$ molecules and the excessive Si atoms are driven to precipitate at the liquid–solid interface. It is worth to mention that the growth temperature and SiCl$_4$ partial pressure have been optimized to obtain vertical Si nanowires with smooth surface and minimum silicon deposition on the nanowire sidewalls. The synthesized Si nanowires were typically 1–25 μm in length, which can be controlled by
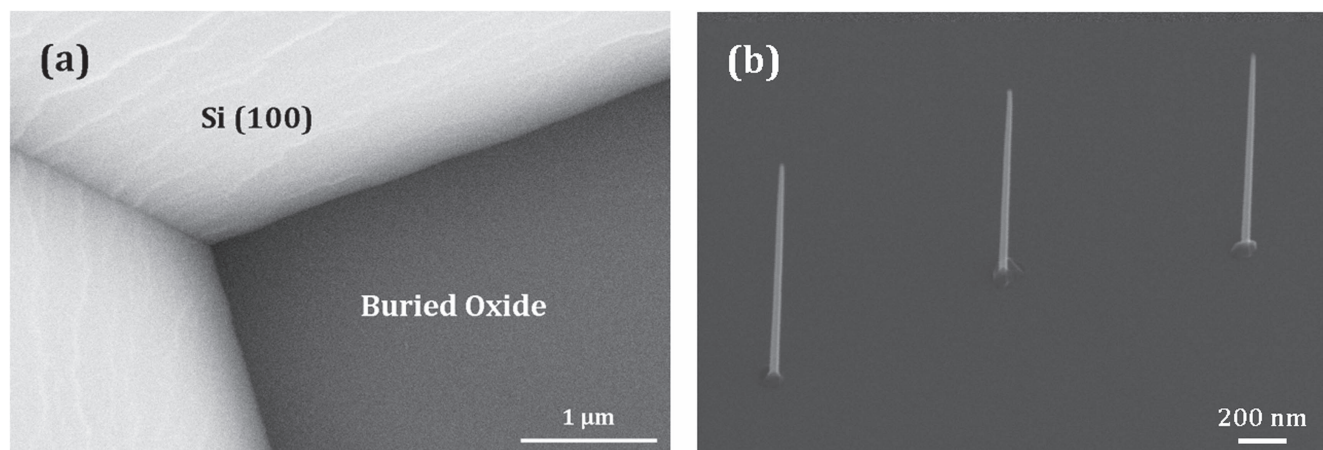
Figure 2. (a) SEM image of buried oxide surface in the cavity into Si (100) after the KOH etching. (b) SEM image of Au-catalyzed Si nanowires growth.

deposition time. Immediately after the growth step, the substrate was loaded into a dry oxide furnace and the Si nanowires were oxidized at 900 °C for 40 min in pure O_2 to form a layer of high-quality and uniform 20 nm thick SiO_2 shell. The diameter of the as-grown Si nanowires is largely determined by the Au nanoparticle size but it can be further reduced to a desired value by repeating oxidation-HF etching process, enabling SiO_2 nanotubes with controllable inner diameters. The final dry etching of Si nanowire core in the Si/SiO_2 core/shell structure will create the SiO_2 nanotubes.

Before the dry etching of Si nanowire core, the substrate was spin-coated with a layer of photoresist. The thickness of photoresist determined the subsequent nanotube height. Then, a brief RIE O_2 plasma cleaning was performed to remove the photoresist off the surface of core/shell Si/SiO_2 extending above the photoresist level. The Au nanoparticle on the top end of Si nanowire and the exposed SiO_2 shell were etched by gold etchant and HF, respectively. After that, the photoresist was completely removed using acetone. Then, XeF_2 etchant gas was used to selectively remove the Si nanowire cores and the suspended Si (111) layer beneath the nanowire. This finally opens a channel in the 20 nm SiO_2 membrane. We chose to remove the photoresist before the XeF_2 dry etching rather than afterwards because the wet chemical removal of photoresist will leave chemical residue on the inner walls of nanotubes. Thus far, we have successfully obtained a solid, smooth SiO_2 nanotube with a connecting nanochannel on SOI substrates. Such a novel controllable nanostructure is a very clean and robust platform for nanofluidic measurement and device applications.

3. Results and discussion

Figure 2(a) shows a scanning electron microscopy (SEM) image of the buried oxide surface in the cavity after the KOH etching. Pyramidal structure with sharp edges into the 400 μm Si (100) layer was achieved with the highly anisotropic etching. The smooth oxide surface and the clear contrast between the SiO_2 and Si (100) side wall indicate the uniform

and complete anisotropic etching with proper stopping position. After etching and removal of the buried oxide and top Si_3N_4, the substrate was loaded in a CVD reactor for the epitaxial growth of Si nanowires. The Au-catalyzed nanowires were oriented perpendicularly to the Si (111) substrate, forming a well-organized nanowire array. The use of $SiCl_4$ results in the byproduct of gaseous hydrogen chloride (HCl), which can etch the oxide layer on the Si surface during reaction. As described before, we have optimized the growth parameters including temperature and $SiCl_4$ partial pressure to obtain a majority of nanowires growing in the vertical $\langle 111 \rangle$ direction on a Si (111) surface. Figure 2(b) shows an example of the as-grown nanowires with 80 nm diameter and 4 μm length. After the growth of nanowires, we performed multiple oxidation-etching processes to thin down the nanowire diameter, subsequently leading to smaller nanotubes. The nanotube height was limited by the thickness of photoresist layer coated following the step of nanowire oxidation. In this step, photoresist was used instead of parylene as reported by Fan *et al* [18]. This is because photoresist is harder and more uniform on the substrate than parylene, and it can be easily removed with a chemical solution by the conventional clean CMOS process without the risk of damaging or contaminating the nanowire surface. After removal of photoresist and XeF_2 etching, free-standing SiO_2 nanotubes have been successfully obtained. Figure 3(a) shows the cross-sectional SEM image of a nanotube after the removal of the whole Si nanowire core and part of the Si (111) layer by XeF_2 etching. The nanotube has a uniform inner diameter of 30 nm with a smooth 20 nm SiO_2 wall. Such a smooth SiO_2 wall surface is a result of the high-quality dry oxidation. The hemisphere shape of etched cavity in Si (111) beneath the nanotube indicated that the XeF_2 etching of Si is isotropic. It should be noted that the as-grown Si nanowires and the fabricated SiO_2 nanotubes tended to be tapered, which can be seen in both figures 2(b) and 3(a). Such a tapering of Si nanowires has been ascribed to the gradual decrease of the catalytic droplet diameter, as well as the etching by the byproduct HCl during nanowire growth [22–24].
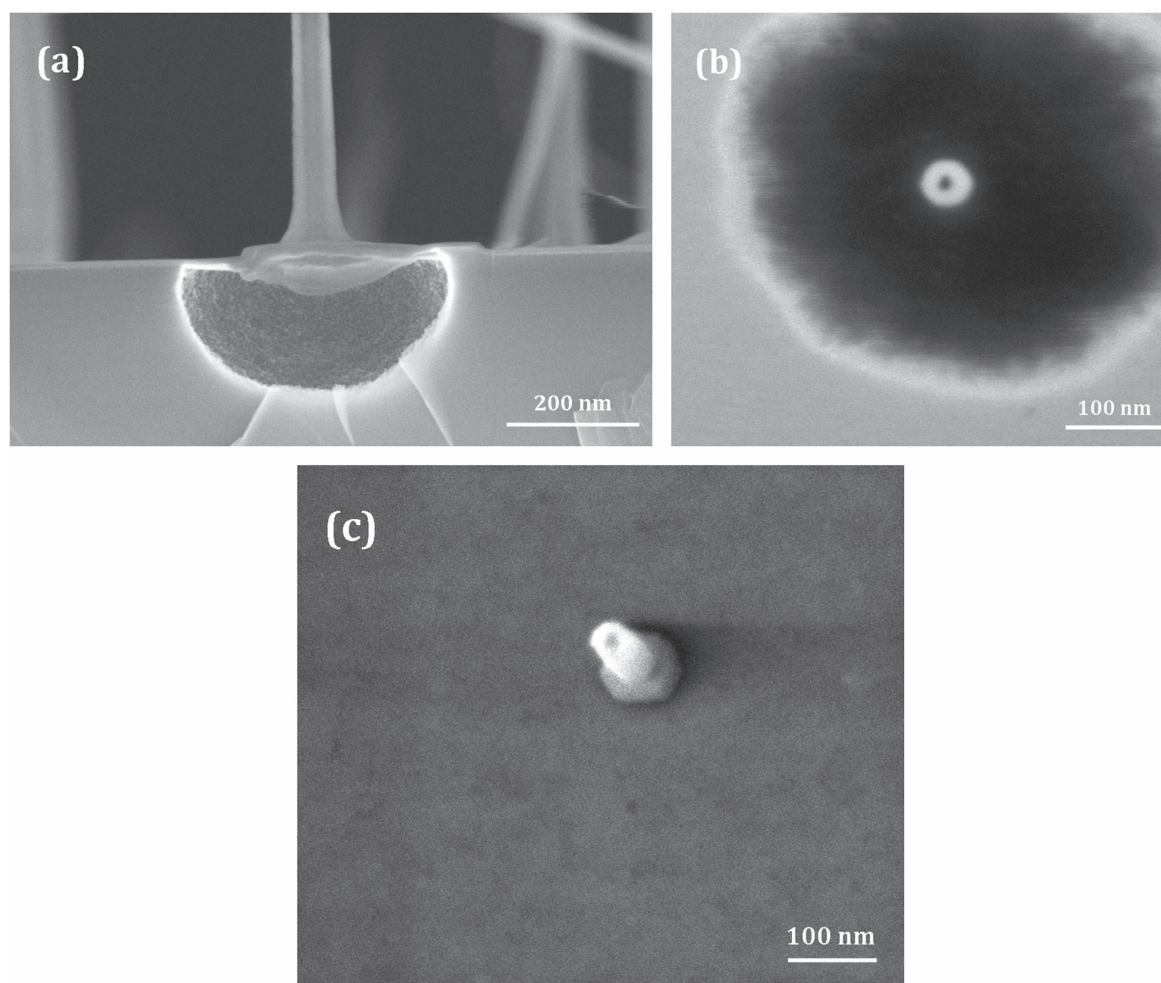
Figure 3. (a) Cross-sectional SEM image of a nanotube on SOI substrate during XeF$_2$ etching before thrilling through Si (111) layer. (b) Non-tilted and (c) tilted top view of a fabricated nanotube (a different sample from the one illustrated in (a)) with about 500 nm height and 20 nm inner diameter standing on the 20 nm thick rigid SiO$_2$ membrane.

Further XeF$_2$ etching will remove the remaining SOI under the SiO$_2$ nanotubes. As shown in figures 3(b) and (c), a free-standing nanotube with ≈20 nm inner diameter and 20 nm thick SiO$_2$ wall maintained the original size and morphology (a different sample from the one illustrated in figure 3(a)). The 20 nm SiO$_2$ membrane with an area of 0.2 μm^2 is strong enough to sustain the nanotube without cleaving. As observed in figure 3(c), the height of nanotubes is about 500 nm, and the hexagonal base of the nanotube derived from the original shape of Si nanowires. Since the inner diameter and the thickness of SiO$_2$ nanotube wall can be precisely controlled by dry oxidation process, these solid-state inorganic nanotubes are rigid and smooth, which is attractive for the nanofluidic system applications. In addition, the SiO$_2$ inner and outer nanotube surfaces obtained in this work are readily applicable for various surface functionalization and modifications, which will be of great significance in future chemical-/bio-sensing applications. Another advantage of the SiO$_2$ nanotube over other materials such as Si$_3$N$_4$ nanotubes or even carbon nanotubes is that the SiO$_2$ tubes are inherently hydrophilic, making it wet easily in various chemical- or bio-

sensing applications. Preliminary conductance measurements suggest that the nanoparticle dispersion method can produce membranes with a small number (i.e., less than three) of unobstructed nanotubes on the membrane (see supplementary information, available online at stacks.iop.org/NANO/28/435601/mmedia).

Critical to the development of scalable nanofluidic devices, our nanotube preparation did not involve focused ion beam which will heavily increase the cost and is not applicable for large batch fabrication, or milling process which will inevitably introduce contaminants and damage to the nanochannel. Eliminating the costly, serial fabrication steps offers a route to routine manufacturability of such nanofluidic devices. Additionally, our nanotube on SOI paradigm gives rise to *in situ* cell fabrication without nanotube harvesting and aligning on target substrates. Therefore, simultaneous batch fabrication of nanotube arrays is possible with our approach. Attempts have been made to grow epitaxial Si nanowires from patterned Au catalyst on SOI substrates. Au pads with different size were defined with e-beam lithography, and formed by 20 nm deposition with e-beam evaporation and lift-off processes. Figure 4(a) shows the
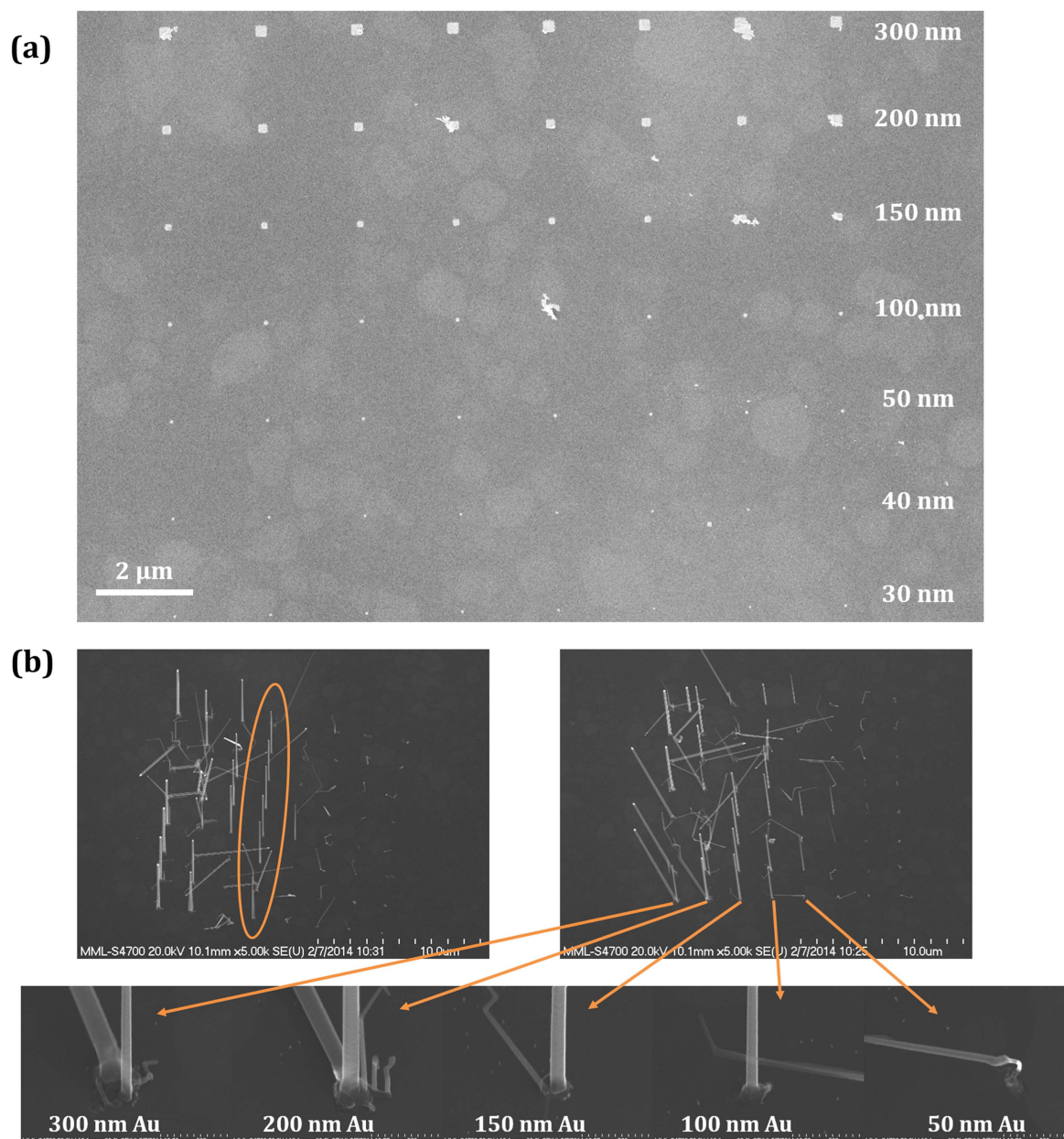
Figure 4. (a) SEM image of the patterned Au catalysts with different pad sizes. The thickness of the Au pads is 20 nm. (b) Tilted top-view of the Si nanowires grown from the patterned Au catalysts. Optimal nanowire morphology has been observed for the 100 nm size Au pads.

patterned Au catalyst with different sizes of 300, 200, 150, 100, 50, 40 and 30 nm squares. Then, the substrates were loaded in the same CVD reactor for Si nanowire synthesis. As shown in figure 4(b), nanowires have barely been observed from the 50 nm and smaller Au pads, while for 150 nm and larger pads, the nanowires are much thicker and multiple nanowires were stretched out at most locations. For the growth conditions used in this study, the nanowires with best morphology, vertical alignment, and ~80% yield were produced from the 100 nm Au pads. A complete fabrication for nanotube array from these 100 nm Au pads to realize a more practical nanofluidic system will require further study. Fabrication of vertical arrays of Si nanowires with different diameter can be achieved by tuning the growth parameters.

4. Conclusions

In summary, we developed a novel process of integration of solid-state SiO_2 nanotubes on a SOI substrate which enables *in situ* fabrication of nanofluidic cells from the self-assembled SiO_2 nanotubes without dispersion/aligning. This is attractive for large-scale integration of clean devices with rigid, uniform and high-quality oxide wall, and a hydrophilic and smooth surface. The inner diameter of the nanotube can be precisely controlled through multiple oxidation-etching steps. With further position-controlled nanowire growth using a self-assembly plus lithography integration technology, batch fabrication of nanotube arrays can be realized. Such a new and optimized nanofabrication process to enable well controlled

SiO$_2$ nanotubes for advanced nanofluidic device/system applications are very attractive for bio-medical application.

Acknowledgments

References

[1] Kasianowicz J J, Brandin E, Branton D and Deamer D W 1996 *Proc. Natl Acad. Sci. USA* **93** 13770
[2] Howorka S, Cheley S and Bayley H 2001 *Nat. Biotechnol.* **19** 636
[3] Li J, Stein D, McMullan C, Branton D, Aziz M J and Golovchenko J A 2001 *Nature* **412** 166
[4] Siwy Z, Trofin L, Kohli P, Baker L, Trautmann C and Martin C R 2005 *J. Am. Chem. Soc.* **127** 5000
[5] Lee S B, Mitcell D T, Trofin L, Nevanen T K, Soderlund H and Martin C R 2002 *Science* **296** 2198
[6] Kiani K 2014 *Acta Mech.* **225** 3569
[7] Goldberger J, He R R, Zhang Y F, Lee S W, Yan H Q, Choi H J and Yang P D 2003 *Nature* **422** 599
[8] Kiani K 2014 *Physica* E **60** 229
[9] Kiani K 2014 *Curr. Appl. Phys.* **14** 1116
[10] Kiani K 2014 *Physica* B **449** 164
[11] Saleh O A and Sohn L 2003 *Nano Lett.* **3** 37
[12] Mitchell D T, Lee S B, Trofin L, Li N C, Nevanen T K, Soderlund H and Martin C R 2002 *J. Am. Chem. Soc.* **124** 11864
[13] Storm A J, Chen J H, Ling X S, Zandbergen H W and Dekker C 2003 *Nat. Mater.* **2** 537
[14] Kohli P, Harrell C C, Cao Z H, Gasprarc R, Tan W H and Martin C R 2004 *Science* **305** 984
[15] Martin C R 1996 *Chem. Mater.* **8** 1739
[16] Kovtyukhova N I, Mallouk T E and Mayer T S 2003 *Adv. Mater.* **15** 780
[17] Bechelany M, Amin A, Brioude A, Cornu D and Miele P 2012 *J. Nanopart. Res.* **14** 980
[18] Fan R, Wu Y, Li D, Yue M, Majumdar A and Yang P 2003 *J. Am. Chem. Soc.* **125** 5254
[19] Fan R, Karnik R, Yue M, Li D, Majumdar A and Yang P 2005 *Nano Lett.* **5** 1633
[20] Bean K E 1978 *IEEE Trans. Electron Devices* **25** 1185
[21] DelRio F W, White R M, Krylyuk S, Davydov A V, Friedman L H and Cook R F 2016 *Nanotechology* **27** 31LT02
[22] Krylyuk S, Davydov A V and Levin L 2011 *ACS Nano* **5** 656
[23] Givargizov E I and Sheftal N N 1971 *J. Cryst. Growth* **9** 326
[24] Bae J, Kulkarni N N, Zhou J P, Ekerdt J G and Shih C K 2008 *J. Cryst. Growth* **310** 4407